Sound propagation through the Antarctic Convergence Zone and comments on three major experiments

Marshall V. Hall

Emeritus Scientist, DSTO Sydney, Pyrmont NSW, Australia

ABSTRACT

Long-range hydroacoustic propagation at low frequencies is determined by: (a) the sound velocity profile (SVP) of the ocean as a function of depth and position on the spheroidal geoid, (b) seafloor topography, and (c) the acoustic properties of the seabed. Neglecting transverse refraction, an acoustic path follows a great ellipse on the geoid. The Antarctic Convergence Zone (ACZ) defines a front between two water masses with different types of SVPs. It is circumpolar and its latitude varies between –60° and -50°. The path from an acoustic pulse emitted in high southern latitudes to a hydrophone at a temperate latitude is likely to cross the ACZ. This is expected to change the shape of the signal and increase its dispersion and complexity. For Transmission Loss (TL) along a path that crosses the ACZ, it is expected that there would be no discontinuity in TL at the ACZ, but there would be a discontinuity in the rate of change of TL with range. There have been three major experiments that have involved propagation through the ACZ: (1) Perth to Bermuda in March 1960, (2) Project Neptune (Cape Town to New Zealand) in April 1964, and (3) the Heard Island Feasibility Test in January 1991. For the first two, which involved the firing of shots, both the sources and receiver were north of the ACZ so there were two crossings of the zone. For the third, the projector (which emitted tones near a frequency of 57 Hz) was located within the ACZ, so there was a partial one-way crossing. The results of these experiments have been reviewed, and it is concluded that the observed signal shape and TL are broadly consistent with the expectations listed above.

THE ACOUSTIC ENVIRONMENT

General features

Hydroacoustic propagation at low frequencies is determined by:

- the sound velocity profile (SVP) of the ocean as a function of depth. It varies with season and position on the geoid [but is usually written as a function of depth, V(z)],
- the seafloor topography, and
- the acoustic properties of the seabed.

The sound source and receiver are assumed to be points in the ocean (as distinct from within the seabed or onshore). Sound waves reflect from the sea surface (almost perfectly) and from the seafloor. The ocean is thus an acoustic waveguide, albeit with varying thickness and properties.

For ranges (R) comparable with the earth mean radius (R_E) of 6370 km, the ocean is more correctly modelled as a spherical shell than as a flat layer, since rays cease diverging horizontally and will reconverge as they approach the antipode of their source. The cylindrical spreading loss of 10 log (R) should be replaced by 10 log [R_E sin (R/R_E)] (McDonald et al, 1994). For $R < R_E$, the loss approximates the flat earth value of 10 log (R). For a range of R_E for example, the difference is 0.8 dB. At the antipodes, the convergence effect would be reduced somewhat due to refraction by transverse "horizontal" variations in V or seafloor depth (SFD) dispersing the rays over a finite region.

The effect of earth curvature on the vertical dependence of the sound field can be allowed for by increasing the depth gradient of V by $V(0)/R_E$.

The SVP is determined primarily by the temperature profile and depth, and to a lesser degree by variations in salinity. Sound velocity varies with ocean properties as follows (Mackenzie, 1981):

- with temperature at a rate of around 4 m/s/C°. dV/dT decreases from 4.5 m/s/C° at 0° C to 2.0 m/s/C° at 30° C.
- with depth at a rate of around 0.017 /s. dV/dz increases from 0.016 /s at the surface to 0.018 /s at depths around 5 km.
- with salinity at a rate of 1.3 m/s /ppt (salinity is reported in parts per thousand, ppt).

In the ocean between Antarctica and Cape Leeuwin for example, the temperature varies between 1° and 20° C, depths of interest range between 0 and 5 km, and salinity varies between 33.7 and 35.6 ppt. The corresponding variations in sound velocity are 70 m/s, 85 m/s, and 2 m/s, respectively.

The Antarctic Convergence Zone (ACZ)

The ACZ defines a front between two water masses with different types of SVPs. It is a circumpolar front whose latitude varies between –60° and -50°. At latitudes of at least 5° north of the ACZ there is typically an isothermal surface mixed layer above a thermocline over which the temperature drops from its maximum value to around 1° or 2°C. The thermocline extends over the depth interval from around 0.1 km to 1 km. Typical values of the sea surface temperature are 5°C at –50° latitude, 20°C at –35°, and 30°C between –10° and the equator. From 1 km to the seafloor, the water is quasi-isothermal. South of the ACZ the water is quasi-isothermal from the surface to the seafloor, except during the austral summer (Jan – Mar) when there may be a small

thermocline. During the summer the sea surface temperature may change by 7 C degrees across the ACZ, which is of the order of 300 km wide (Kibblewhite et al, 1977). The effect of this variation is that:

- for latitudes at least 5° north of the ACZ, V(z) has a minimum at a depth of 1 to 1.3 km
- as latitude approaches the ACZ the depth of the SVP minimum shallows and approaches the surface
- south of the ACZ, the SVP minimum is at the surface.

Providing it is submerged, the SVP minimum is referred to as the SOFAR axis.

SVPs at latitudes from –65° to –35° (along the 115° meridian) have been computed by applying the Mackenzie (1981) formula to summer and winter temperature and salinity profiles. These profiles were obtained from the World Ocean Atlas (1998), using averages over 5-degree squares. The summer results are shown in Figure 1, and the winter results are shown in Figure 2 (no result was available for latitude -60° in winter). It can be seen that the average latitude of the ACZ at this meridian lies between –50° and -45°.

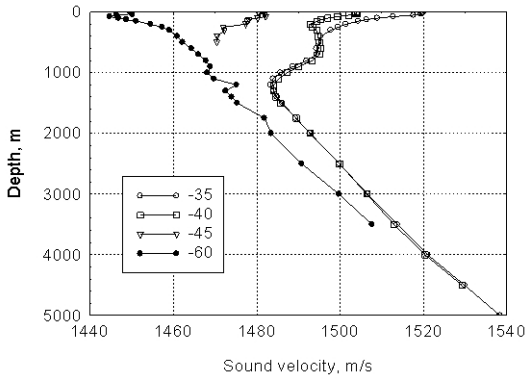

Figure 1. Summertime sound velocity profiles on the 115° meridian. Numeral in legend is latitude.

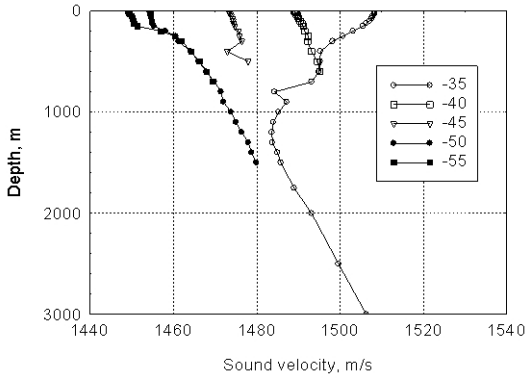

Figure 2. Wintertime sound velocity profiles on the 115° meridian.

The bathymetry along the 114-deg. Meridian between Australia and Antarctica was obtained from the ETOPO2 database (National Geophysical Data Center, n.d.), and is shown in Figure 3. This meridian was chosen since the hydrophone station installed by the Comprehensive Test Ban Treat Organisation (CTBTO) at Cape Leeuwin is close to it. The position of the right-hand end of the curve is between Cape Leeuwin and Cape Naturaliste. The SFD is generally greater than 4 km, and the "Southeast Indian Ridge" can be seen at -50° latitude, where the SFD decreases to 3 km.

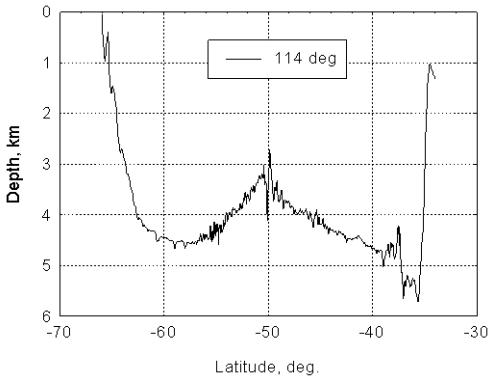

Figure 3. Seafloor depth along the 114° meridian between Antartica and south Western Australia.

In addition to geographic variations in SVP and SFD, the property of seawater that affects long-distance propagation is chemical absorption. At frequencies above 5 kHz absorption is primarily due to Magnesium Sulphate and seawater viscosity. At lower frequencies it becomes primarily due to boric acid (Yeagher et al, 1973), and increases somewhat with alkalinity (pH). In seawater at 5° C and pH = 8.1 (typical of the ACZ), the absorption coefficient increases from 0.1 to 1 dB /1000 km as frequency increases from 30 to 100 Hz. The average ocean pH is 8.0. An increase of 0.1 increases the absorption coefficient by 20%.

To some investigators in the 1970s (Kibblewhite et al, 1977, for example), the measured TL seemed to be greater than that predicted by conventional propagation algorithms and absorption, and they attributed this to scattering by microstructure in the SVP. The contrary hypothesis is that the loss was due entirely to the boundaries (sea-surface and seabed). Sea-surface roughness causes scattering away from the specular direction, and the resulting loss increases with both grazing angle and frequency. Such loss may be significant south of the ACZ, since the surface is usually rough and, due to the low sound velocity there, horizontally travelling sound rays reflect from the surface at vertical grazing angles up to several degrees (depending on the SFD; rays sufficiently steep to reflect off the seafloor are generally negligible). The loss from the specular reflection due to roughness is given by (Tolstoy & Clay, 1966, page 206):

$$RL\ (dB) = 20\ /\ln(10) \times (2\ k\ \sigma \sin\theta)^2$$

where k is the wavenumber ($2\ \pi\ f\ /C$), σ is the RMS surface roughness, and θ is the grazing angle. For a typical wind speed of 20 knots, the RMS roughness is 0.55 m (Chapman, 1983). For an angle of 5° (which corresponds to a SFD of around 350 m) and frequency of 100 Hz, the resulting loss is 0.01 dB per bounce. In a surface layer with a constant sound velocity gradient (g), the rays are circular arcs and the skip distance between reflections is $2\ \rho \sin\theta$, where ρ is the radius of curvature ($\rho = C/g = 91$ km). At an angle of 5° the skip distance between surface bounces in an isothermal layer is 16 km, so the long range attenuation rate is of the order of 1 dB per 1000 km.

North of the ACZ the sound waves are mostly trapped in the submerged SOFAR channel and are not affected by surface roughness. For a shallow source and receiver, Bannister and Pedersen (1981) found that long-range propagation exhibits a "surface decoupling" loss that increases as the frequency decreases.

If SFD is sufficiently small that TL is determined by seabed reflections (c. 2 km, say), a propagation algorithm that includes shear velocity will yield a higher TL than one that does not, since some waterborne energy is lost in the generation of shear waves in the seabed. Neglect of the shear velocity (characterizing the seabed as a liquid) was a common assumption in the 1960s and 70s.

Publications on long-range propagation in the past 20 years have chosen to ignore microstructure, and have attributed measured TLs to the boundaries, together with absorption and refraction due to large-scale changes in SVP.

CALCULATING TRANSMISSION LOSS

For a given source position, there are four types of algorithms for computing TL at any position in an ocean:

1. Direct integration of the Bessel transform of the Greens function
2. Normal modes
3. Parabolic equation (PE)
4. Rays

Range-independent waveguides

For each of these types, the simplest waveguide is one in which the acoustic properties and SFD are independent of range (a range-independent waveguide). Since the SVP varies only with depth, the 3-D wave equation for sound pressure can be separated into independent (uncoupled) differential equations in two orthogonal co-ordinates: either the cylindrical co-ordinates of range and depth, or the spherical co-ordinates of radius and arc-length. For this case, the algorithms can be very accurate. The wave-number integration method is exact, the normal mode method is exact (except over the source), the PE method is highly accurate (except for phase errors at long ranges), and the ray method (which neglects diffraction) is accurate at high frequencies, other than in shadow zones or caustics.

For all types, the calculated TL will contain two standard terms:

- Spreading Loss (as described above)
- Attenuation Loss

Spreading Loss is determined by the SVP and the large-scale seafloor topography. An upward refracting SVP or a SOFAR channel renders the SFD less important, while a downward refracting SVP accentuates the role of the SFD.

Attenuation Loss is determined by the reflectivity and roughness of each boundary, and the SVP. (An upward refracting SVP accentuates the role of the sea-surface, while a downward refracting SVP accentuates the role of the seafloor. A SOFAR channel will render both boundaries less important.) This term asymptotes to a linear increase with range, and the rate of increase is called the attenuation coefficient. In a range-independent waveguide this coefficient will be constant.

Range-dependent waveguides

Algorithms of each of the above four types have also been developed for waveguides whose acoustic properties or SFD vary with range. Judging by publications on long-range low-frequency propagation over the past 15 years, the most popular are PE and adiabatic-modes.

For propagation through the ACZ, the important variation with range is that of the SVP, both in the magnitude of V and the shape of its profile. Along some sections across the ACZ the SFD is typically between 4 and 5 km and is not changing rapidly. For such sections, characterising TL across the ACZ may be addressed with the assumption of a constant SFD. On other sections of the ACZ the seafloor can be shallow, due to islands and banks. Important examples are Heard and Macdonald Islands near longitude 74°, Banzare Bank near 78°, Mill Bank near 148°, and Macquarie Island at 160°. Near such features, TL across the ACZ will be determined by the bathymetry and the acoustic properties of the seabed.

For a range-dependent waveguide there can be a sudden change in TL. For example, consider a hypothetical ocean divided into two homogeneous halves by a thin vertical plane front, and a propagation path orthogonal to the front. As the sound wave crosses the front, some energy is reflected back toward the source, and TL as a function of range will have a discontinuity there. A receiver on the same side as the source will detect a reflection after the direct arrival, and the energy of this will increase the discontinuity. Any disparity in the SVP across a front may cause these effects to occur. In the real ocean, the reflection and discontinuity will occur but their amplitudes will be small, since the thickness of a front is much greater than the sound wavelength.

For northward propagation from a source south of the ACZ, the attenuation coefficient will drop to a lower value as the receiver crosses the ACZ, due to the removal of the rough sea-surface as a boundary of the waveguide. The spreading loss may increase somewhat, since in the SOFAR channel the wave front will extend over a greater depth interval than it did in the isothermal channel.

CALCULATING TRAVEL TIME

In principle each of the four types of transmission algorithm may be used to compute travel time (TT) of an emitted pulse. Most algorithms do computations one frequency at a time. Although called TL algorithms, they also compute the "complex" sound pressure (from which the magnitude and phase are obtained).

Fourier synthesis

A method that can be used with any algorithm has three steps:

- compute the complex pressure at the receiver at a sequence of equally spaced frequencies over the band that defines the spectrum of the emitted transient. To obtain a reasonable graphical display, a sampling rate of 8 times the highest frequency in the signal has been recommended (Jensen et al, 1994, page 483)
- Fourier synthesise the results to produce the received pulse signal
- observe the travel time of a particular feature of that pulse (usually its peak).

The frequency spacing would be set to the reciprocal of the estimated time spread of the received signal. For long-range propagation, the time spread can be around 20 s. For a signal with frequency content up to 100 Hz, this process would thus require the TL algorithm to be run at 2000 frequencies up to

100 Hz, and the pressures at frequencies from 100 to 800 Hz would be padded with zeroes.

Mode group velocity

A simpler method is to use adiabatic mode theory, and the group velocities (GV) of the modes at a single frequency. This method invokes adiabatic mode theory to include refraction due to transverse variations in the horizontal phase velocities (PV) of the modes. These results include separate horizontal paths for each of the modes that are considered to be potentially significant, using an archival data set of ocean SVPs and topography to generate the modes numerically. This yields a grid of PV(x,y) and GV(x,y), where x and y denote longitude and latitude. The significant modes are selected as those whose amplitudes at the receiver are similar to the maximum modal amplitude. The TTs are then obtained by integrating the reciprocal of GV of the significant modes along the 2-D propagation paths.

Ray theory

A method that is simple in principle, but can be complicated in practice, is to determine the rays that emanate from the source and pass through the receiver. The rays that yield the maximum amplitude at the receiver would be selected. Their travel times are calculated by integrating the reciprocal of V(x,y,z) along the 3-D ray paths.

THE THREE EXPERIMENTS

There have been three major experiments that have involved propagation through the ACZ:

During March 1960, three explosive shots were fired off Perth and received near Bermuda (Shockley et al, 1982). Analysis yielded travel times and wideband signal-to noise ratios (SNR) at the two hydrophones monitored.

Project Neptune: in April 1964 an aircraft fired 18 underwater shots between Cape Town and Perth. These were monitored with a hydrophone off southern New Zealand, on the edge of the shelf at a depth of 0.11 km (Kibblewhite et al, 1965). Analysis yielded travel times and signal energies at frequencies from 12.5 Hz to 200 Hz in third-octave steps.

The Heard Island Feasibility Test (HIFT): in January 1991 a projector emitted tones near 57 Hz for five days (Munk and Baggeroer, 1994). The projector appears to have been in the ACZ since the sound velocity at the surface was 1.46 km/s (which corresponds to a temperature of 2° C), and the SOFAR axis there was 0.18 km deep (Munk et al, 1994). SFD was 1.0 km. The October 1994 issue of the Journal of the Acoustical Society of America (volume 96, no. 4) contains 17 papers that describe experimental and theoretical aspects of receptions at the 10 sites where useful signals were received. Analyses yielded travel times and either signal intensity (for calibrated hydrophones) or SNR (for uncalibrated hydrophones).

Transmission Loss

Perth-Bermuda: The measured signal for each shot of the Perth-Bermuda experiment contained two pulses (separated by 30 s). An analysis with adiabatic mode theory at 15 Hz concluded that there were two primary paths, both 20 Mm in length (Heaney et al, 1991). The shorter path "A" did not cross the ACZ and was unimpeded by interaction with the seafloor. The longer path "B" crossed the ACZ in both directions and was slightly impeded by the seafloor near Brazil. The theoretical TL for B was 7 – 12 dB greater than for A (attributed to seabed attenuation), while the observed difference was 10 dB. The effect of the ACZ on TL thus appears to have been negligible.

Neptune: The TL results were found to be much larger than obtained for propagation over similar ranges (up to 9900 km) at temperate latitudes. This was attributed to the absence of a thermocline south of the ACZ.

HIFT: The closest monitoring site was Kerguelen Island (670 km NNW), where the TL estimated from SNR was 107 dB (Birdsall et al, 1994). The average SFD along the path was 0.5 km, and there would have been no SOFAR channel along most of the path. With no SOFAR channel, the theoretical TL for a non-reflecting seabed would be spherical spreading. Allowing some decrease due to reflections from the seafloor yields TL < 60 + 10 log (670 x 670) = 116 dB. For an average SFD of 0.5 km, the theoretical TL for a perfectly reflecting seafloor would be cylindrical spreading. Allowing some increase due to reflection being imperfect yields TL > 60 + 10 log (0.5 x 670) = 85 dB. With the seafloor this shallow, TL would be determined by the unknown reflectivity of the seabed, and it is unlikely that effects of the ACZ could be isolated.

The next closest site was Christmas Island (5490 km NNE), where the estimated TL was 125 dB one day, and 115 dB the next. The SFD was greater than 3 km most of the path, except where it decreased to 1.7 km on the S.E. Indian Ridge (at -42°) and to 0.8 km on a ridge named "Broken Plateau" (-32°). With this topography, TL would be affected by the unknown reflectivity of the seabed and it is unlikely that any effect of the ACZ on TL could be isolated.

Travel time

Perth-Bermuda: Whereas the observed difference in TT between the two pulses was 30 s, adiabatic mode theory at 15 Hz yielded a difference between paths A and B of 49 s (Heaney et al, 1991). It seems that the ACZ or the seabed interaction had effects on TT that were not allowed for by adiabatic mode theory.

Neptune: The signal envelopes were found to differ in shape from the usual SOFAR case, some having two peaks. This was attributed to the absence of a SOFAR channel over much of the propagation paths.

HIFT: The propagation of acoustic modes over the 9140-km underwater path to Ascension during the Heard Island Feasibility Experiment has been simulated (Shang et al, 1994). Using a modal decomposition of the parabolic-equation field, it was found that mode coupling at the circumpolar front (the ACZ) has significant impact on modal dispersion and modal repopulation, which complicates the pulse-arrival sequence.

CONCLUSIONS

In each of the three experiments, either the source or receiver, or both, were in positions such that along the propagation path the SFD was at some places less than 1 km. Consequently the measured TL would have been affected by the seabed as well as the ACZ. Nevertheless the data may prove useful for comparison with algorithms, once the effect of the seabed has been incorporated.

REFERENCES

Bannister, R. W., & Pedersen M. A. 1981, "Low-frequency surface interference effects in long-range sound

propagation", *Journal of the Acoustical Society of America* vol. 69, pp. 76-83.

Birdsall, T. G., Metzger, K., & Dzieciuch, M. A. 1994, "Signals, signal processing, and general results", *Journal of the Acoustical Society of America* vol. 96, pp. 2343-2352.

Chapman, D. M. F. 1983, "An improved Kirchhoff formula for reflection loss at a rough surface at low grazing angles", *Journal of the Acoustical Society of America* vol. 73, pp. 520-527.

Heaney, K. D., Kuperman, W. A., & McDonald, B. E. 1991, "Perth-Bermuda sound propagation (1960): adiabatic mode interpretation", *Journal of the Acoustical Society of America* vol. 90, pp. 2586-2594.

Jensen, F. B., Kuperman, W. A., Porter, M. B., & Schmidt, H. 1994, "Computational ocean acoustics", American Institute of Physics, New York.

Kibblewhite, A. C., Denham, R. N., & Barker, P. H. 1965, "Long range sound propagation study in the Southern Ocean – Project Neptune", *Journal of the Acoustical Society of America* vol. 38, pp. 629-643.

Kibblewhite, A. C., Shirtcliffe, T. G., & Stanton, B. R. 1977, "Effects of temperature microstructure on low-frequency propagation in the South Tasman Sea", *Journal of the Acoustical Society of America* vol. 62, pp. 308 – 319.

McDonald, B. E., Collins, M. D., Kuperman, W. A., & Heaney, K. D. 1994, "Comparison of data and model predictions for Heard Island acoustic transmissions", *Journal of the Acoustical Society of America,* vol. 96, pp. 2357 – 2370.

Mackenzie, K. V. 1981, "Nine term equation for sound speed in the oceans", *Journal of the Acoustical Society of America* vol. 70, pp. 807 – 812.

Munk, W. H. & Baggeroer, A. 1994, "The Heard Island papers: a contribution to global acoustics", *Journal of the Acoustical Society of America* vol. 96, pp. 2327-2329.

Munk, W. H., Spindel, R. C., Baggeroer, A., & Birdsall, T. G. 1994, "The Heard Island Feasibility Test", *Journal of the Acoustical Society of America* vol. 96, pp. 2330-2342.

National Geophysical Data Center n.d. Retrieved: April 2005, from http://www.ngdc.noaa.gov/mgg/gdas/gd_designagrid.html

Shang, E. C., Wang, Y. Y., & Georges, T. M. 1994, "Dispersion and repopulation of Heard–Ascension modes", *Journal of the Acoustical Society of America* vol. 96, pp. 2371-2379.

Shockley, R. C., Northrop, J., Hansen, P. G., & Hartdegen, C. 1982, "SOFAR propagation paths from Australia to Bermuda: Comparison of signal speed algorithms and experiments", *Journal of the Acoustical Society of America* vol. 71, pp. 51-60.

Tolstoy, I. & Clay, C. S. 1987, "Ocean Acoustics", Second edition, American Institute of Physics, New York.

"World Ocean Atlas 1998 (Online Data)" 1998. Retrieved July 2004, from http://www.nodc.noaa.gov/OC5/data_woa.html

Yeager, E., Fisher, F. H., Miceli, J., & Bressel, R. 1973, "Origin of the low-frequency sound absorption in seawater", *Journal of the Acoustical Society of America* vol. 53, pp. 1705 – 1707.